Transilvania University of Brasov

FACULTY OF MECHANICAL ENGINEERING

IN ASSOCIATION WITH:

ACADEMY OF TECHNICAL SCIENCES OF ROMANIA

ROMANIAN SOCIETY OF THEORETICAL AND APPLIED MECHANICS

THE ROMANIAN ACOUSTIC SOCIETY

The 7th International Conference on "Advanced Composite Materials Engineering" – COMAT 2018

The 42th International Conference on "Mechanics of Solids, Acoustics and Vibrations" – ICMSAV 2018

The 2nd International Conference "Experimental Mechanics in Engineering" – eMECH 2018

ISSN 2457 – 8541
ISSN-L 2457 - 8541

Brașov, ROMANIA, 25- 26 October 2018

Contents ICMSAV 2018 & COMAT 2018 & eMECH 2018

Transilvania University of Brasov
FACULTY OF MECHANICAL ENGINEERING
ICMSAV2018 & COMAT2018 & eMECH2018
Brasov, ROMANIA, 25-26 October 2018

STABILITY OF FGM ARCHES UNDER AN ARBITRARY RADIAL CONCENTRATED LOAD

László Péter Kiss[1], **György Szeidl**[2]
[1,2]Institute of Applied Mechanics, University of Miskolc, Miskolc, HUNGARY
mechkiss@uni-miskolc.hu, gyorgy.szeidl@uni-miskolc.hu

***Abstract*:** It is well-known that the mechanical behaviour of shallow arches is strongly nonlinear. Geometrically linear models overestimate the critical (buckling) load and are unable to describe the post-buckling behaviour. In recent years, numerous new findings were published in this topic. We hereby intend to contribute by presenting and evaluating a new mechanical model for the case when pinned-pinned arches, made of functionally graded material, are subject to an arbitrary concentrated radial dead load.
Keywords: *nonlinear stability, circular arch, FGM, snap-through buckling, bifurcation buckling*

1. INTRODUCTION

Arches (or curved beams) have an important role in many engineering structures, e.g., in roof structures or in bridges. Research on the mechanical behaviour of these structural elements began in the 19 th century -- see [1] by Love. The most important results achieved before the sixties of the last century are presented in [2] by Timoshenko and Gere. Based on a geometrically nonlinear analytical model, solutions for homogeneous, uniform shallow arches subjected to a vertical load at the crown point are provided in [3,4] by Bradford et al. Recent results for non-uniform members can be found e.g., in [5,6] by Jin et al. Using equilibrium approach, Bradford et al. have also tackled the issue when a homogeneous pinned-fixed arch is subject to arbitrary radial (dead) load [7]. After reviewing the open literature, we have found that the nonlinear planar stability of functionally graded (FG) pinned-pinned circular arches under arbitrary concentrated radial load is still an open issue. In this paper we assume that the radius of curvature is constant and the Young modulus depends on the cross sectional coordinates only. We aim to derive and evaluate a refined, geometrically nonlinear Euler-Bernoulli beam model to reveal the effect of the load position on the behaviour of the structural element.

2. MECHANICAL MODEL

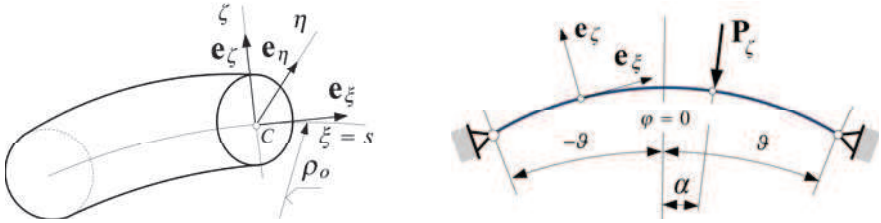

Figure 1: (a) The coordinate system, (b) The centerline with the external load and supports

Figure 1a shows a portion of the arch considered; the orthogonal curvilinear coordinate system $(\xi\eta\zeta)$ - $\eta = \zeta = 0$ on the (E -weighted) centerline with radius ρ_o and the unit vectors $\mathbf{e}_\xi$, $\mathbf{e}_\eta$ and $\mathbf{e}_\zeta$. The cross-section of the arch is symmetric with respect to the axis ζ . The point in which the centerline intersects the cross-section is denoted by C . Its position on the cross-section follows from the condition

$$Q_{e\eta} = \int_A E(\eta,\zeta)\zeta dA = 0 \qquad (1)$$

#

where $Q_{e\eta}$ is the E-weighted first moment with respect to the axis η. The Young modulus satisfies the relation $E(\eta,\zeta)=E(-\eta,\zeta)$. The arc coordinate s is measured from the crown point while $\varphi=s/\rho_o$ is the angle coordinate. The displacement vector at an arbitrary point on the cross-section takes the form

$$\mathbf{u}=\mathbf{u}_o+\psi_{o\eta}\zeta\mathbf{e}_\xi=w_o\mathbf{e}_\zeta+(u_o+\psi_{o\eta}\zeta)\mathbf{e}_\xi,\quad \psi_{o\eta}=u_o/\rho_o-dw_o/ds, \tag{2}$$

where $\mathbf{u}_o=u_o\mathbf{e}_\xi+w_o\mathbf{e}_\zeta$ and $\boldsymbol{\psi}=\psi_{o\eta}\mathbf{e}_\eta$ are the displacement and rotation on the centerline. It can be shown that the axial strain is

$$\varepsilon_\xi=(1+\zeta/\rho_o)^{-1}(\varepsilon_{o\xi}+\zeta\kappa_o)+\psi_{o\eta}^2/2 \quad \text{in which} \tag{3a}$$

$$\varepsilon_{o\xi}=\frac{du_o}{ds}+\frac{w_o}{\rho_o},\quad \frac{d\psi_{o\eta}}{ds}=\kappa_o=-\frac{d}{ds}\left(\frac{dw_o}{ds}-\frac{u_o}{\rho_o}\right)\quad\text{and}\quad \varepsilon_m=\varepsilon_{o\xi}+\frac{1}{2}\psi_{o\eta}^2. \tag{3b}$$

Here $\varepsilon_{o\xi}$ and ε_m are the linear and nonlinear axial strains on the centerline while κ_o is the change of curvature. We assume that $\sigma_\xi=E(\eta,\zeta)\varepsilon_\xi$ is the Hooke law. We will apply the following two notational conventions in the forthcoming:

$$\rho_o^n d^n(\ldots)/ds^n=d^n(\ldots)/d\varphi^n=(\ldots)^{(n)},\ n=1,2,\ldots;\ m=A_e\rho_o^2/I_{e\eta}. \tag{4}$$

Making use of the Hooke law we get the bending moment and the axial force as

$$M=\int_A E\varepsilon_\xi\zeta dA\cong -I_{e\eta}\left(w_o^{(2)}+w_o\right)/\rho_o^2,\ N=\int_A E\varepsilon_\xi dA\approx A_e\varepsilon_m-I_{e\eta}\kappa_o/\rho_o; \tag{5}$$

here A_e and $I_{e\eta}$ are the E-weighted area and the E-weighted moment of inertia:

$$A_e=\int_A E dA;\quad I_{e\eta}=\int_A E\zeta^2 dA. \tag{6}$$

It can be checked by applying the kinematic equations that

$$\psi_{o\eta b}=u_{ob}/\rho_o-dw_{ob}/ds;\ \ \varepsilon_{\xi b}=(1+\zeta/\rho_o)^{-1}(\varepsilon_{o\xi b}+\zeta\kappa_{ob})+\psi_{o\eta}\psi_{o\eta b}+\psi_{o\eta b}^2/2; \tag{7}$$

where the subscript $_b$ denotes the increment of the various physical quantities between the pre-buckling and post-buckling states. It can also be shown that

$$M_b\approx -I_{e\eta}\left(w_{ob}^{(2)}+w_{ob}\right)/\rho_o^2\ \text{ and }\ N_b\approx A_e\varepsilon_{mb}-M_b/\rho_o. \tag{8}$$

3. PRE- AND POST-BUCKLING EQUILIBRIUM EQUATIONS

Figure 1b shows the centerline of the arch in the initial configuration. The loading consists of a concentrated radial dead force $P_\zeta(\varphi=\alpha)$. The central angle of the beam is 2ϑ. For the pre-buckling state equation

$$\int_V \sigma_\xi\delta\varepsilon_\xi dV=P_\zeta\delta w_o\big|_{\varphi=\alpha} \tag{9}$$

is the principle of virtual work from where we can get the equilibrium equations

$$\frac{dN}{ds}+\frac{1}{\rho_o}\left[\frac{dM}{ds}+\left(N+\frac{M}{\rho_o}\right)\chi_o\right]=0,\ \ \frac{d}{ds}\left[\frac{dM}{ds}+\left(N+\frac{M}{\rho_o}\right)\chi_o\right]+\frac{N}{\rho_o}=0. \tag{10}$$

Let us substitute relation $(5)_2$ for the force N into $(10)_1$. What remains is $(A_e\varepsilon_m)^{(1)}-(A_e\varepsilon_m\psi_{o\eta})/\rho_o=0$. Since the product $\varepsilon_m\psi_{o\eta}$ is quadratic in the displacements it can be neglected. Therefore we arrive at the equation

$$\varepsilon_m^{(1)}=0\ \rightarrow\ \varepsilon_m=\text{constant}. \tag{11}$$

Manipulations on $(10)_2$ are not detailed, only the final form is presented:

$$W_o^{(4)}+\left(2+\chi^2-1\right)W_o^{(2)}+\underline{\chi^2 W_o}=\chi^2-1,\ \ W_o=w_o/\rho_o,\ \ \chi^2=1-m\varepsilon_m. \tag{12}$$

This equation can be compared to that published by Bradford et al. in their series of articles -- see, e.g., equation (14) in [3]. The cited authors have dropped the underlined terms. The principle of virtual work in the buckled equilibrium state assumes the form

$$\int_V \sigma_\xi^*\delta\varepsilon_\xi^* dV=-P_\zeta^*\delta w_o^*\big|_{\varphi=\alpha}. \tag{13}$$

Here the asterisk symbol denotes the sum of the change between the initial and the pre-buckling configuration (not remarked specifically) and the increment to the post-buckling equilibrium state (denoted by $_b$) -- e.g.,

#

$\varepsilon_m^* = \varepsilon_m + \varepsilon_{mb}$. Eq. (13) coincides formally with (9). After some manipulations (the details are again omitted) it can be shown that the arbitrariness of the virtual quantities yield the following post-buckling equilibrium equations:

$$\begin{aligned} &\frac{d}{ds}\left(N_b + \frac{M_b}{\rho_o}\right) - \frac{1}{\rho_o}\left(N + \frac{M}{\rho_o}\right)\psi_{o\eta b} - \frac{1}{\rho_o}\left(N_b + \frac{M_b}{\rho_o}\right)\psi_{o\eta b} = 0\,, \\ &\frac{d^2 M_b}{ds^2} - \frac{N_b}{\rho_o} - \frac{d}{ds}\left[\left(N + \frac{M}{\rho_o} + N_b + \frac{M_b}{\rho_o}\right)\psi_{o\eta b} + \left(N_b + \frac{M_b}{\rho_o}\right)\psi_{o\eta}\right] = 0, \end{aligned} \tag{14}$$

The structure of equilibrium equation $(14)_1$ is very similar to that of $(10)_1$ except that the last term in $(14)_1$ does not appear in the pre-buckling relation. However, it can be neglected since this product is quadratic in the increments. Therefore, repeating the same line of thought resulting in $(10)_1$ but now for the increments it follows that

$$\left(A_e \varepsilon_{mb}\right)^{(1)} - \left(A_e \varepsilon_m \psi_{o\eta b}\right)/\rho_o = 0 \;\rightarrow\; \varepsilon_{mb}^{(1)} = 0 \;\rightarrow\; \varepsilon_{mb} = \text{constant}\,. \tag{15}$$

Manipulations on equilibrium equation $(14)_2$ are more complicated and are neglected. The final form is relation (16). Compared to the model of Bradford et al. it is more accurate via the presence of the underlined terms -- see equation (39) in [3].

$$W_{ob}^{(4)} + (\underline{2} + \chi^2 - 1)W_{ob}^{(2)} + \underline{\chi^2 W_{ob}} = m\varepsilon_{mb}\left[1 - W_o^{(2)} - \underline{W_o}\right],\;\; W_{ob} = w_{ob}/\rho_o. \tag{16}$$

4. SOLUTION TO THE PRE-BUCKLING STATE

The pre-buckling equilibrium is governed by equations (11) and (12). Due to the discontinuity in the shear force at $\varphi = \alpha$, the solutions are sought separately on the left $(-\vartheta;\alpha)$ and right $(\alpha;\vartheta)$ sides as

$$W_{ol} = \frac{\chi^2 - 1}{\chi^2} + A_1 \cos\varphi + A_2 \sin\varphi - \frac{A_3}{\chi^2}\cos\chi\varphi - \frac{A_4}{\chi^2}\sin\chi\varphi\,,\; A_i \in \mathbb{R}, \tag{17}$$

$$W_{or} = \frac{\chi^2 - 1}{\chi^2} + B_1 \cos\varphi + B_2 \sin\varphi - \frac{B_3}{\chi^2}\cos\chi\varphi - \frac{B_4}{\chi^2}\sin\chi\varphi\,,\; B_i \in \mathbb{R}. \tag{18}$$

The integration constants A_i, B_i can be determined by utilizing the boundary, continuity and discontinuity conditions gathered in Table 1.

Table 1: Pre-buckling boundary and (dis)continuity conditions

$W_{ol}\big\vert_{\varphi=-\vartheta} = 0$	$W_{or}\big\vert_{\varphi=\vartheta} = 0$
$W_{ol}^{(2)}\big\vert_{\varphi=-\vartheta} = 0$	$W_{or}^{(2)}\big\vert_{\varphi=\vartheta} = 0$
$W_{ol}\big\vert_{\varphi=\alpha} = W_{or}\big\vert_{\varphi=\alpha}$	$W_{ol}^{(1)}\big\vert_{\varphi=\alpha} = W_{or}^{(1)}\big\vert_{\varphi=\alpha}$
$W_{ol}^{(2)}\big\vert_{\varphi=\alpha} = W_{or}^{(2)}\big\vert_{\varphi=\alpha}$	$-W_{ol}^{(3)}\big\vert_{\varphi=\alpha} + W_{or}^{(3)}\big\vert_{\varphi=\alpha} = \frac{P_\zeta \rho_o^2 \vartheta}{2I_{e\eta}}$

At the supports the displacement and the bending moment are zero. At α the typical fields are continuous except the shear force. The jump in the shear force has a magnitude P_ζ . Altogether, there are eight equations for eight unknowns. After solution, with the normal displacement in hand, the rotation can be calculated as $\psi_{o\eta} = U_o - W_o^{(1)} \approx -W_o^{(1)}$. Here we have assumed that the tangential displacement has negligible effect on the rotation field due to the shallowness. Since the axial strain is constant on the centerline, we can calculate it as its mathematical average:

$$\varepsilon_m = \frac{1}{2\vartheta}\int_{-\vartheta}^{\vartheta} \varepsilon_m(\varphi)\,d\varphi = I_1 + I_2 \mathbf{P} + I_3 \mathbf{P}^2, \text{with} \tag{19}$$

$\mathbf{P} = (-P_\zeta \rho_o^2 \vartheta)/(2I_{e\eta})$ being the dimensionless load. The integration constants I_1, I_2, I_3 can be given in closed-form.

5. SOLUTIONS TO THE POST-BUCKLING STATE

#

After substituting the solution to the pre-buckling displacement into the right side of equation (16), for the left ($_l$) and right ($_r$) sides we get that

$$W_{ob\,l}^{(4)} + (1+\chi^2)W_{obl}^{(2)} + \chi^2 W_{obl} = \varepsilon_{mb}\frac{1-\nu^2}{m}\left(\frac{1}{1-\nu^2}A_3\cos m\varphi + A_4\sin m\varphi\right), \tag{20}$$

$$W_{obr}^{(4)} + (1+\chi^2)W_{obr}^{(2)} + \chi^2 W_{obr} = \varepsilon_{mb}\frac{1-\nu^2}{m}\left(\frac{1}{1-\nu^2}B_3\cos m\varphi + B_4\sin m\varphi\right). \tag{21}$$

Given that ε_{mb} is constant, it can be averaged as

$$\varepsilon_{mb} = \frac{1}{2\vartheta}\int_{-\vartheta}^{\vartheta}\left(U_{ob}^{(1)} + W_{ob} + \psi_{o\eta b}\psi_{o\eta}\right)d\varphi. \tag{22}$$

It is possible that $\varepsilon_{mb} \neq 0$ =constant, then we have to solve equation (21) and if $\varepsilon_{mb} = 0$ we get the homogeneous equation

$$W_{ob}^{(4)} + (1+\chi^2)W_{ob}^{(2)} + \chi^2 W_{ob} = 0 \tag{23}$$

which follows from (21). It is also important to mention that after buckling every physical quantity is continuous through the interval $\varphi \in [-\vartheta;\vartheta]$ because there is no increment in the loading. The general solutions of equations (20)-(21) take the form

$$W_{obr} = D_1\cos\varphi + D_2\sin\varphi + D_3\sin(\chi\varphi) + D_4\cos(\chi\varphi) - \frac{m\varepsilon_{mb}}{2\chi^3}\left(\frac{2}{\chi} + B_3\varphi\sin(\chi\varphi) - B_4\varphi\cos(\chi\varphi)\right), \tag{24}$$

$$W_{obl} = C_1\cos\varphi + C_2\sin\varphi + C_3\sin(\chi\varphi) + C_4\cos(\chi\varphi) - \frac{m\varepsilon_{mb}}{2\chi^3}\left(\frac{2}{\chi} + A_3\varphi\sin(\chi\varphi) - A_4\varphi\cos(\chi\varphi)\right) \tag{25}$$

with $C_i, D_i \in \mathbb{R}$, while the displacement satisfying relation (23) is sought in the form

$$W_{ob}(\varphi) = E_1\cos\varphi + E_2\sin\varphi + E_3\sin\chi\varphi + E_4\cos\chi\varphi; \quad E_i \in \mathbb{R}. \tag{26}$$

Considering $\varepsilon_{mb} = 0$ (bifurcation buckling), after substituting solution (26) into the boundary conditions (BCs) in Table 2, we arrive at a homogeneous system of linear equations for which nontrivial solution exists if the determinant of the coefficient matrix is zero:

$$\mathbb{D} = (1-\chi)^2(1+\chi)^2\sin\chi\vartheta\cos\chi\vartheta\cos\vartheta\sin\vartheta = 0. \tag{27}$$

Recalling the relation $\chi^2 = 1 - m\varepsilon_m$; we can come to the conclusion that there is only one physically possible solution that is $\sin\chi\vartheta = 0 \rightarrow \chi = \pi/\vartheta$ thus

$$\varepsilon_m = \frac{1}{m}\left(1-\chi^2\right) = \frac{1}{m}\left[1-\left(\frac{\pi}{\vartheta}\right)^2\right] \tag{28}$$

is the lowest (critical) strain. If we now substitute this solution back to the equation system we can check that $E_1 = E_2 = E_4 = 0$. Consequently, it follows from the general solution (26) that the shape of the beam is antisymmetric when $\varepsilon_{mb} = 0$ since

$$W_{ob}(\varphi) = E_3\sin\frac{\pi}{\vartheta}\varphi. \tag{29}$$

However, when $\alpha \neq 0$, bifurcation buckling can not occur since the radial displacement increments are orthogonal to the pre-buckling displacements [7]. Therefore

$$\frac{1}{2\vartheta}\int_{-\vartheta}^{\vartheta} W_{ob}d\varphi \neq 0 \tag{30}$$

because this displacement increment is unsymmetrical along the arch.

#

Table 2: Post-buckling boundary and continuity conditions

$W_{obl}\big\|_{\varphi=-\vartheta} = 0$	$W_{obr}\big\|_{\varphi=\vartheta} = 0$
$W^{(2)}_{obl}\big\|_{\varphi=-\vartheta} = 0$	$W^{(2)}_{obr}\big\|_{\varphi=\vartheta} = 0$
$W_{obl}\big\|_{\varphi=\alpha} = W_{obr}\big\|_{\varphi=\alpha}$	$W^{(1)}_{obl}\big\|_{\varphi=\alpha} = W^{(1)}_{obr}\big\|_{\varphi=\alpha}$
$W^{(2)}_{ol}\big\|_{\varphi=\alpha} = W^{(2)}_{obr}\big\|_{\varphi=\alpha}$	$W^{(3)}_{ol}\big\|_{\varphi=\alpha} = W^{(3)}_{obr}\big\|_{\varphi=\alpha}$

When the strain increment is nonzero (snap-through buckling), substitution of the related solutions into the boundary conditions of Table 2 yields an inhomogeneous system of equations, which can be solved in closed-form. With W_{ob}, the rotation increment is $\psi_{o\eta b} \approx -W^{(1)}_{ob}$ if we again neglect the effect of the tangential displacement on the angle of rotation. Now equation (22) can be rewritten as

$$\varepsilon_{mb} = \frac{1}{2\vartheta}\int_{-\vartheta}^{\vartheta}\left(W_{ob} + W_o^{(1)}W_{ob}^{(1)}\right)d\varphi. \tag{31}$$

If we now substitute all the previously determined kinematical quantities into the above equation, perform the integration and simplify by the increment ε_{mb}, we get

$$1 = J_1 + J_2\mathbf{P} + J_3\mathbf{P}^2 \rightarrow \hat{J}_1 + J_2\mathbf{P} + J_3\mathbf{P}^2 = 0\,, \quad J_i \in \mathsf{R}. \tag{32}$$

Here each of the constants J_i can be expressed in closed-form.

6. COMPUTATIONAL RESULTS

We can find the critical load for bifurcation buckling when we plug the critical strain (28) into Eq. (19). For snap-through buckling, we have to solve nonlinear equations (19) and (32) simultaneously for the two unknowns: the critical strain and critical load. When the load is a central one ($\alpha = 0$), results of the current model coincide with those published in [8].

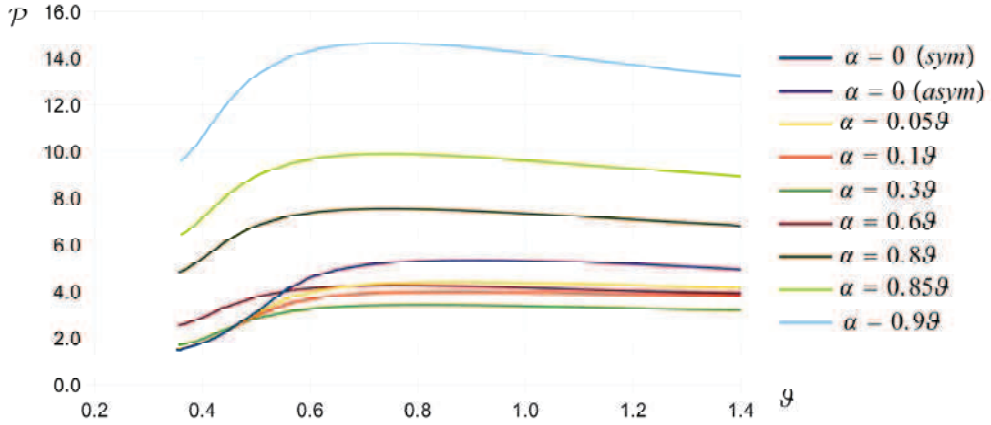

Figure 2: Critical dimensionless load in terms of the semi-vertex angle

Numerical results are provided for $m = 10^3$. As can be seen from Figure 2, when $\alpha = 0$, for a short while snap-through buckling is dominant with symmetric (sym) buckled shape, but from $\vartheta > 0.55$, bifurcation buckling occurs first with antisymmetric (asym) shape. A small perturbation in the position of the external load makes the buckling load decrease sensibly if $\vartheta > 0.5$ (yellow and orange curves). So we may say that the structural element is sensitive to small loading imperfections. Further, when $\alpha = 0.3\vartheta$ or 0.6ϑ, for smaller central angles the critical load is greater than originally ($\alpha = 0$). If we move the position of the external load even closer to either end-support, the load carrying capabilities are much better than in the original setup.

#

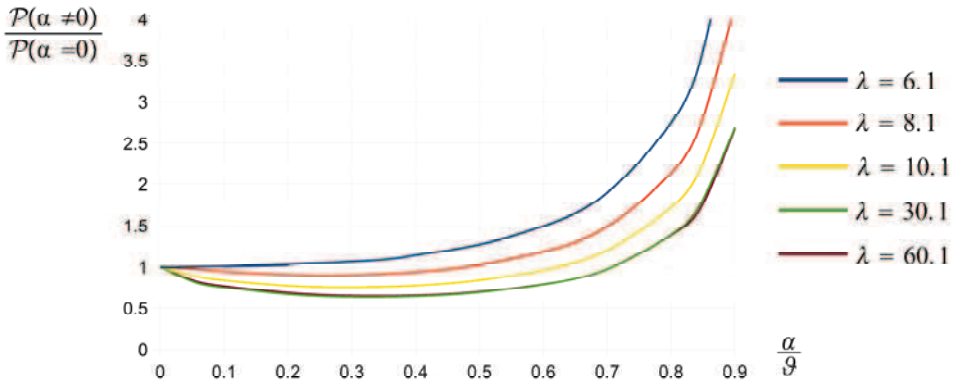

Figure 3: The effect of the external load position on the buckling load

In Figure 3, we investigate how the position of the concentrated load affects the critical load for some selected geometries. Here $\lambda = \sqrt{m}\vartheta^2$ is the modified slenderness of the arch. When $\lambda = 6.1$ the buckling load continuously increases as we move the external load away from the crown point. Interestingly, for all other geometries, at first, the load carrying capability shows (an occasionally) considerable decrease but after that, if α is sufficiently great, there is an increase up to a multiple times of the initial load.

Table 3: Finite element verifications

α	$P / P_{(Abaqus)}$ if $\lambda = 4.9$	$P / P_{(Abaqus)}$ if $\lambda = 43.9$
0	0.98	1.01
0.1	1.01	1.02
0.25	1.02	1.06
0.5	1.03	1.10
0.75	1.06	1.13

Validations were also carried out using Abaqus CAE 13 with B21 beam elements and the Riks step on geometrically nonlinear models. The cross-section of the arch was uniform, square with a typical dimension of 10 mm. The material was linearly elastic with E=200,000 MPa. Numerical results are shown in Table 3. The correlations confirm the validity of our model.

7. CONCLUDING REMARKS

For pinned-pinned functionally graded arches, we have set up and evaluated a geometrically nonlinear model for in-plane stability investigations provided that the arch is subjected to an arbitrary concentrated radial force. We remark that our kinematical model is more accurate than that presented in [3,4]. We have found that the position of the external force has significant effect on the buckling load. The critical load either continuously increases with the load position angle α or first decreases, and then shows an increase. Certain geometries seem to be sensitive to small loading imperfections.

Acknowledgements: This research was supported by the National Research, Development and Innovation Office – NKFIH, K115701.

REFERENCES

[1] A. E. H. Love. *A Treatise on the Mathematical Theory of Elasticity I. and II*. Cambridge University Press, 1892.
[2] S. P. Timoshenko and J. M. Gere. *Theory of Elastic Stability*. Engineering Society's Monographs. McGraw-Hill, 2nd edition, 1961.
[3] Y. L. Pi, M. A. Bradford, and B. Uy. In-plane Stability of Arches. *International Journal of Solids and Structures*, 39:105–125, 2002.
[4] B. Uy M. A. Bradford and Y-L. Pi. In-plane elastic stability of arches under a central concentrated load. *Journal of Engineering Mechanics*, 128(7):710–719, 2002.

[5] S. t. Yan, X. Shen, Z. Chen, and Z. Jin. On buckling of non-uniform shallow arch under a central concentrated load. *International Journal of Mechanical Sciences*, 133:330–343, 2017.
[6] S. t. Yan, X. Shen, Z. Chen, and Z. Jin. Collapse behavior of non-uniform shallow arch under a concentrated load for fixed and pinned boundary conditions. *International Journal of Mechanical Sciences*, 137:46–67, 2018.
[7] A. Liu, M. A. Bradford, and Y.-L. Pi. In-plane nonlinear multiple equilibria and switches of equilibria of pinned-fixed arches under an arbitrary radial concentrated load. *Archive of Applied Mechanics*, 87:1909–1928, 2017.
[8] L. Kiss and Gy. Szeidl. Nonlinear in-plane stability of heterogeneous curved beams under a concentrated radial load at the crown point. *Technische Mechanik*, 35(1):1–30, 2015.

#